°C for 2.5 days the solvent was removed (VRE) and the residue chromatographed on silica with benzene–pyridine 9:1 and 7:1 to afford the triisoxazole **4α** (0.66 g, 31%) as an amorphous foam (the unconverted CD was recovered quantitatively). The minor impurities were removed by a second chromatography on silica with 100% EtOAc to give 0.51 g (24%) of **4α**: $[\alpha]^{25}_{D}$ −6.1°, $[\alpha]^{25}_{435}$ −16.6° (*c* 5.00, CHCl₃); IR (CHCl₃) 2240 (w, C≡N), 1730 (s, C=O, ester), 1635 (m, C=O, amide), 1585 (m, C=C, isox.), 1550 cm⁻¹ (m, NO₂); ¹H NMR (CDCl₃) δ 1.11 (s, 3 H, CH₃, ring A), 1.29, 1.31, 1.33 (s, 6 H + 3 H + 3 H, 4 × CH₃, ring A, C, D), 1.65 (s, 3 H, CH₃ ring B), 1.70–3.45 (m, 26 H, 11 × CH₂ + 4 × CH), 2.84 and 2.92 (s, each 3 H, NMe₂), 3.60, 3.62, 3.64, 3.71 (s, total 15 H, 5 × CH₃O), 3.75–4.05 (m, 4 H, OCH₂CH₂O), 4.37 and 4.45 (ABX, *J*ₐᵦ = 14, *J*ₐₓ = 7.5, *J*ᵦₓ = 4.5, each 1 H, CH₂NO₂), 5.72, 5.920, 5.925 (s, each 1 H, 3 × CH, isox.); ¹³C NMR (CDCl₃) δ 177.82 and 175.78 (2 × C—O, isox.), 173.64, 173.29, 173.16, 173.00, 172.81, 171.50 (5 × C=O ester, C—O isox.), 169.36 (C=O, amide), 164.13, 163.52, 162.95 (3 × C=N, isox.), 118.71 (C≡N), 113.35 (O—C—O), 103.48, 102.97, 101.34 (3 × CH, isox.), 76.57 (CH₂NO₂), 64.86, 63.10 (OCH₂CH₂O), 52.28, 51.58 (intense, 2C), 51.42, 51.13 (5 × CH₃O), 48.07, 46.51, 45.80, 43.09, 41.59 (intense, 3C)*, 39.90, 38.94, 37.60, 36.52, 35.43, 33.74, 33.10, 32.30, 32.17, 32.05, 25.66, 24.83, 24.64, 24.23, 23.88, 21.90, 21.77, 18.93, 18.80, 12.70 (CH₂CN); MS (FAB), *m/z* 1071 (MH⁺); *two of the three superimposed peaks at δ 41.59 also overlap in CD at δ 41.62, the third missing signal is only visible in the diastereomer **4β**. Anal.: C, 58.27; H, 6.83; N, 7.87. Calcd for C₅₂H₇₄N₆O₁₈: C, 58.31; H, 6.96; N, 7.85%.

Triisoxazole 4β. The procedure was the same as for the triisoxazole **4α** using AB*β* instead to yield **4β** (0.53 g, 25%): $[\alpha]^{25}_{D}$ +3.4°, $[\alpha]^{25}_{435}$ +2.3° (*c* 2.82, CHCl₃); ¹H NMR (CDCl₃) δ 1.15 (s, 3 H, CH₃, ring A),

1.31, 1.32, 1.34, 1.37 (s, each 3 H, 4 × CH₃, ring A, C, D), 1.55 (s, 3 H, CH₃, ring B), 1.70–3.30 (m, 26 H, 11 × CH₂, 4 × CH), 2.78 and 2.87 (s, each 3 H, NMe₂), 3.60, 3.62, 3.63, 3.71 (s, total 15 H, 5 × CH₃O), 3.75–4.05 (m, 4 H, OCH₂CH₂O), 4.35 and 4.45 (ABX, *J*ₐᵦ = 14, *J*ₐₓ = 7.5, *J*ᵦₓ = 4.5, each 1 H, CH₂NO₂), 5.88, 5.92, 6.03 (s, each 1 H, 3 × CH, isox.); ¹³C NMR (CDCl₃) δ 178.14 and 175.72 (2 × C—O, isox.), 173.61, 173.35, 173.00, 172.90, 172.75, 171.50 (5 × C=O ester, C—O isox.), 169.40 (C=O, amide), 164.29, 163.46, 162.82 (3 × C=N, isox.), 118.71 (CN), 113.38 (O—C—O), 103.48 (br, 2C) and 101.50 (3 × CH, isox.), 76.45 (CH₂NO₂), 64.92 and 63.23, (OCH₂CH₂O), 52.25, 51.61, 51.52, 51.42, 51.13 (5 × CH₃O), 48.17, 46.51, 45.13, 43.12, 41.72 (intense, 2C), 41.59, 41.24, 39.13, 37.73, 36.68, 35.40, 33.71, 33.13, 32.33, 32.24, 32.08, 25.31, 24.93, 24.83, 24.51, 24.26, 21.55, 19.82, 19.06, 18.96, 12.70 (CH₂CN); IR and MS are identical with those of **4α**.

Supplementary Material Available: Tables of final atomic coordinates, bond lengths and angles, and anisotropic thermal parameters along with a computer generated plot with atom labels (11 pages). Ordering information is given on any current masthead page.

Single-Crystal EXAFS of Nitrogenase

A. M. Flank,† M. Weininger,‡ L. E. Mortenson,§ and S. P. Cramer*§

Contribution from the Corporate Research Science Labs, Exxon Research and Engineering Company, Annandale, New Jersey 08801, LURE Batiment 209C, 91405 Orsay, France, and the Department of Biological Chemistry, Purdue University, West Lafayette, Indiana 47907. Received November 19, 1984

Abstract: Single crystals of the nitrogenase Mo–Fe protein have been examined by polarized X-ray absorption spectroscopy. For different orientations, the Mo–Fe amplitude of the Mo K-edge EXAFS was found to change by a factor of 2.5, whereas the Mo–S component varied by only ±15%. The orientation dependence of the EXAFS spectra has been used to investigate the geometry and orientation of the Mo, Fe, S clusters within the Mo–Fe protein. This represents the first application of single-crystal EXAFS to an enzyme of unknown crystal structure. The orientation dependence for single crystals of the model compounds (Ph₄P)₂[Cl₂FeS₂MoS₂FeCl₂] and (Et₄N)₃[Fe₆Mo₂S₈(SEt)₉] was also examined to quantify the experimental precision of this technique. The analysis procedures overcome the difficulty of four molybdenum sites per unit cell by using the X-ray diffraction evidence for a crystallographic 2-fold axis and a molecular 2-fold axis. Given initial assumptions about the symmetry of the Mo, Fe, S clusters, as well as the orientation of one cluster with respect to the crystallographic axes, it was possible to calculate the expected EXAFS orientation dependence. The patterns for linear, bent, tetrahedral, and square-pyramidal symmetries in various orientations were then compared with the experimental spectra. It was found that the experimental data were not well simulated by clusters with a linear arrangement of Fe–Mo–Fe atoms, whereas trinuclear clusters with a Fe–Mo–Fe angle between 50° and 130° gave satisfactory agreement. Tetrahedral MoFe₃ and square-pyramidal MoFe₄ cluster symmetries also gave satisfactory simulations of the orientation dependence. Assuming a tetrahedral Mo–Fe geometry, the preferred orientation of the 3-fold axis of one of the Mo–Fe clusters was found to lie at an angle of 75 ± 10° from the crystallographic *a* axis and 215 ± 10 or 285 ± 10° from the *b* axis.

Most of the nitrogen fixation on earth is accomplished through the catalytic action of the enzyme nitrogenase.[1] This enzyme consists of two proteins, the Fe protein and the Mo–Fe protein. The Mo–Fe protein is an α₂β₂ tetramer with a molecular weight of 220000 that contains 2 molybdenums, 28–32 irons,[2,3] and approximately 30 acid labile sulfides.[4] An unusual molybdenum–iron–sulfur cluster, the iron–molybdenum cofactor or

"FeMo-co", is thought to be at the catalytic site of this complex.[2]

The first technique that revealed information about the molybdenum site in nitrogenase was X-ray absorption spectroscopy.[5,6]

---

*To whom correspondence should be addressed.
†LURE.
‡Purdue University.
§Exxon Research.

(1) "Current Perspectives in Nitrogen Fixation"; Gibson, A. H., Newton, W. E., Eds.; Australian Academy of Sciences: Canberra, 1981.
(2) Shah, V. K.; Brill, W. J. *Proc. Natl. Acad. Sci. U.S.A.* **1977,** *74,* 3249–3253.
(3) Burgess, B. K.; Jacobs, D. R.; Stiefel, E. I. *Biochim. Biophys. Acta* **1980,** *614,* 196–209.
(4) Orme-Johnson, W. H.; Davis, L. C. "Iron-Sulfur Proteins"; Lovenberg, W., Eds.; Academic Press: New York, 1977; p 15.

Scheme I. Recent Proposals for the Structure of the Nitrogenase Molybdenum Site

I

II

III

IV

V

VI
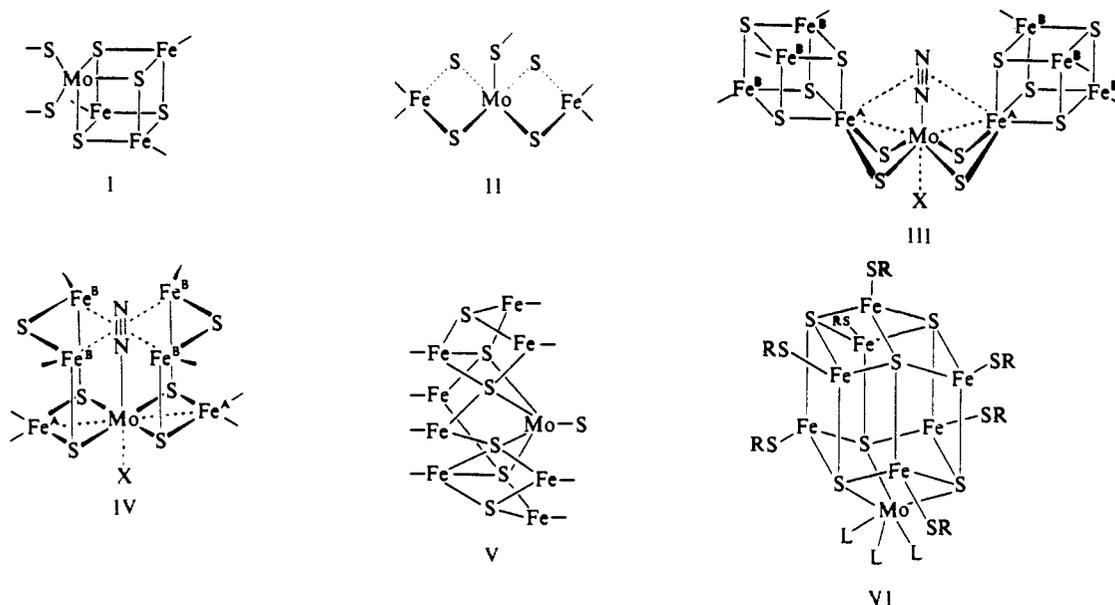
These initial studies deduced the presence of four or five sulfur ligands around the molybdenum, as well as two or three iron atoms in the second coordination sphere.[7,8] Two distinct types of models (I and II) (Scheme I) were originally proposed to account for the EXAFS data,[7] and subsequently other structures (III–VI) for the molybdenum environment have been proposed.[9–13]

The correct stoichiometry of the components of the FeMo-co cluster has been the object of considerable debate. The original composition was reported as $1Mo:8Fe:6(acid-labile)S^{2-}$.[2] Mössbauer spectroscopy on intact Mo–Fe protein yields a minimum value of six irons,[14] while more recent chemical analyses yield seven irons per molybdenum.[15] Sulfur analyses ranging from as low as 4 labile sulfides[15] to as high as 11.9 total sulfurs have been reported.[16]

A wealth of synthetic activity in the area of Mo,Fe,S cluster chemistry has been recently reported,[17–19] and clusters with one, two, or three irons bridged by sulfur to molybdenum have now been synthesized. With the synthesis of FeMo-co as a long-range goal, there still exists uncertainty over even the local structure of the molybdenum site. Some groups have favored the models with three Mo–Fe interactions,[20] while others prefer structures

with only two irons close to the molybdenum.[9,10] Given the ambiguity always associated with EXAFS amplitudes,[21–23] it is unlikely that further conventional EXAFS experiments will unambiguously solve this important structural question.

One means of ending this problem would be the determination of the crystal structure by X-ray diffraction, and work along these lines is in progress.[24,25] Unfortunately, the amount of work involved in solving such a large structure is such that a full structure determination is probably many years away. Furthermore, atomic level resolution of the Mo, Fe, and S positions, while possible, is not guaranteed. However, the same crystals that are being used for the diffraction studies are ideal for another experiment.

Single-Crystal EXAFS.[26] In an X-ray absorption measurement using a K edge or L_1 edge of atom A, the excited state involves a photoelectron p wave emitted from A and oriented along the $\vec{E}$ vector of the X-ray beam. Interference effects generated by the scattering of this wave from neighboring atoms B give rise to the EXAFS oscillations. The EXAFS therefore is sensitive only to those emitter–scatterer interactions with projections along the $\vec{E}$ vector. Quite simply, for a particular EXAFS component, $\chi_{pol}(k) = \chi_{iso}(k)3 \cos^2 \theta$, where χ_{iso} is the EXAFS signal observed on a powder or solution sample, χ_{pol} is the polarized single-crystal EXAFS, k is the photoelectron wave vector, and θ is the angle between the polarization vector and the A–B emitter–scatterer axis. From this equation, the orientation of the A–B axis within the crystal can be obtained from the variation in the amplitude of the A–B EXAFS as a function of crystal orientation. Of course, for complicated structures, these effects have to be summed over all A–B pairs.

The application of this technique to nitrogenase must take into account the facts that the Mo–Fe protein crystals contain four molybdenum atoms per unit cell[24] and that each molybdenum has more than one iron neighbor. This paper describes analysis procedures developed to account for multiple species within the unit cell. Calculations were done for a variety of clusters with different symmetries. Experimental data on single crystals of

(5) Cramer, S. P. "Advances in Inorganic and Bioinorganic Mechanisms"; Sykes, A. G., Eds.; Academic Press: London, 1983; pp 259–316.

(6) Hodgson, K. O.; Hedman, B.; Penner-Hahn, J. E., Eds. "EXAFS and Near Edge Structure III"; Springer-Verlag: Berlin, 1984.

(7) Cramer, S. P.; Hodgson, K. O.; Gillum, W. O.; Mortenson, L. E.; Stiefel, E. I.; Chisnell, J. R.; Brill, W. J.; Shah, V. K. *J. Am. Chem. Soc.* **1978**, *100*, 3398–3407.

(8) Cramer, S. P.; Gillum, W. O.; Hodgson, K. O.; Mortenson, L. E. *J. Am. Chem. Soc.* **1978**, *100*, 3814–3819.

(9) Teo, B. K.; Averill, B. A. *Biochem. Biophys. Res. Commun.* **1979**, *88*, 1454–1461.

(10) Teo, B. K. "EXAFS Spectroscopy: Techniques and Applications"; Teo, B. K., Joy, D. C., Eds.; Plenum Press: New York, 1981; pp 13–58.

(11) Lu, J. "Nitrogen Fixation", Newton, W. E., Orme-Johnson, W. H., Eds.; University Park Press: Baltimore, 1980; pp 343–371.

(12) Tsai, K. R. "Nitrogen Fixation"; Newton, W. E., Orme-Johnson, W. H., Eds.; University Park Press: Baltimore, 1980; pp 373–387.

(13) Christou, G.; Hagen, K. S.; Holm, R. H. *J. Am. Chem. Soc.* **1982**, *104*, 1744–1745.

(14) Rawlings, J.; Shah, V. K.; Chisnell, J. R.; Brill, W. J.; Zimmerman, R.; Münck, E.; Orme-Johnson, W. H. *J. Biol. Chem.* **1978**, *253*, 1001.

(15) Yang, S.-S.; Pan, W.-H.; Friesen, G. D.; Burgess, B. K.; Corbin, J. L.; Stiefel, E. I.; Newton, W. E. *J. Biol. Chem.* **1982**, *257*, 8042–8048.

(16) Nelson, M. J.; Levy, M. A.; Orme-Johnson, W. H. *Proc. Natl. Acad. Sci. U.S.A.* **1983**, *80*, 147.

(17) Averill, B. A. *Struct. Bonding (Berlin)* **1983**, *53*, 59–103.

(18) Garner, C. D.; Acott, S. R.; Christou, G.; Collison, D.; Mabbs, F. E.; Petrouleas, V. *Philos. Trans. R. Soc. London A* **1982**, *308*, 159–166.

(19) Holm, R. H.; Simhon, E. D. "Molybdenum Enzymes"; Spiro, T. G., Ed.; Wiley: New York, 1985; pp 1–87.

(20) Wolff, T. E.; Berg, J. M.; Warrick, C.; Hodgson, K. O.; Holm, R. H.; Frankel, R. B. *J. Am. Chem. Soc.* **1978**, *100*, 4630–4632.

(21) Eisenberger, P.; Lengeler, B. *Phys. Rev. B* **1980**, *22*, 3551–3562.

(22) Cramer, S. P.; Liang, K. S.; Jacobson, A. J.; Chang, C. H.; Chianelli, R. R. *Inorg. Chem.* **1984**, *23*, 1215–1221.

(23) Stern, E. A.; Bunker, B. A.; Heald, S. M. *Phys. Rev. B* **1980**, *21*, 5521–5539.

(24) Weininger, M. S.; Mortenson, L. E. *Proc. Natl. Acad. Sci. U.S.A.* **1982**, *79*, 378–380.

(25) Yamane, T.; Weininger, M. S.; Mortenson, L. E.; Rossman, M. G. *J. Biol. Chem.* **1982**, *257*, 1221–1223.

(26) Hahn, J. E.; Hodgson, K. O. "Inorganic Chemistry: Towards the 21st Century"; Chisolm, M. H., Eds.; American Chemical Society: Washington, D.C., 1983; ACS Symp. Ser. No. 211, pp 431–444.

Single-Crystal EXAFS of Nitrogenase

J. Am. Chem. Soc., Vol. 108, No. 5, 1986 1051

Table I. Curve-Fitting Analysis of Model Compound Single-Crystal EXAFS

sample	orientation	Mo–Fe			Mo–S			Mo–S'		
		N	R, Å	σ, Å^2	N	R, Å	σ, Å^a	N	R, Å	σ, Å^a
$(Et_4N)_3[Fe_6Mo_2S_8(SEt)_9]$	$\hat{E}_\parallel$ 3-fold	4.59	2.70	0.053	1.8	2.37	0.055	2.5	2.57	0.067
$(Et_4N)_3[Fe_6Mo_2S_8(SEt)_9]$	$\hat{E}_\perp$ 3-fold	1.43	2.72	0.053	3.5	2.35	0.055	2.4	2.58	0.067
$(Et_4N)_3[Fe_6Mo_2S_8(SEt)_9]$	(xtal struct.) ref 29	3	2.723 (2)		3	2.347 (3)		3	2.568 (3)	
$(Ph_4P)_2[Cl_2FeS_2MoS_2FeCl_2]$	powder	2	2.77	0.061	4	2.21	0.039			
$(Ph_4P)_2[Cl_2FeS_2MoS_2FeCl_2]$	(xtal struct.) ref 28	2	2.775 (6)	0.061	4	2.204 (5)				
$(Ph_4P)_2[Cl_2FeS_2MoS_2FeCl_2]$	Mo–Fe max	1.84	2.78	0.061	3.9	2.21	0.039			
$(Ph_4P)_2[Cl_2FeS_2MoS_2FeCl_2]$	Mo–Fe min	0.12	2.79	0.061	3.4	2.21	0.039			

^{a} σ was fixed at typical values found for model compounds.

Mo,Fe,S clusters with known structures were also analyzed to check the precision of the experimental procedures. Finally, EXAFS spectra of nitrogenase single crystals were recorded for a number of orientations, and the observed amplitude dependence was used to shed light on the symmetry and orientation of the nitrogenase Mo,Fe,S clusters.

Experimental Section

Sample Preparation. The model compounds [NEt$_4$][S$_2$MoS$_2$Fe-(SPh)$_2$],[27] [Ph$_4$P]$_2$[Cl$_2$FeS$_2$MoS$_2$FeCl$_2$],[28] and [Et$_4$N]$_3$[Fe$_6$Mo$_2$S$_8$-(SEt)$_9$][29] were synthesized and crystallized by published procedures. Nitrogenase Mo–Fe protein from *Clostridium pasteurianum* was crystallized as described previously.[24]

Data Collection. All the spectra were recorded at the Stanford Synchrotron Radiation Laboratory on the wiggler beam line VII-3 during dedicated operation. Fluorescence detection using zirconium filters[30] was used for all samples except the model compound powders, which were examined in transmission mode. In all cases, an internal energy calibration was obtained with a molybdenum foil using a three-ion-chamber geometry.

Since the 1 mm thick protein crystals had very weak absorption at 20 keV, a new procedure was required for optimum sample alignment. A helium–neon laser was used to illuminate the optical path between two narrow tantalum slit assemblies, which were previously adjusted to pass the X-ray beam. The crystals were positioned in the X-ray beam by first centering them visually in the laser beam and then making small adjustments with a stepping motor to maximize the X-ray fluorescence signal.

The orientations of the crystals were obtained from precession photographs. After data collection, the nitrogenase crystals were reexamined for radiation damage. In all cases, the crystals still diffracted to at least 4 Å.

Data Analysis. The spectra were calibrated, processed, and fit by using previously described programs and functions.[31-34] An E_0 of 20025 eV was used for all the spectra. The amplitude function used to describe the Mo–Fe interaction was the backscattering amplitude calculated by Teo and Lee,[35] with a scale factor reduction of 0.39, while the remaining Mo–S and Mo–Fe functions have been reported previously.[33]

The orientation dependence of the EXAFS was calculated by using the simple formula $\chi_{pol}(k) = \chi_{iso}(k)^3 \cos^2 \theta$, as defined previously. For calculations involving nitrogenase crystals, a computer program was written which uses as input the cluster symmetry and the orientation of the first cluster in terms of Eulerian angles α and β, as defined in Figure 5. The orientation of the second cluster is generated by rotation about the molecular 2-fold axis, which has been crystallographically located[25] in the position illustrated in Figure 5. The third and fourth clusters are then generated by rotating the first and second clusters about the crystallographic 2-fold axis. With the orientation of all the clusters defined, the program then calculates the expected relative EXAFS amplitude as

(27) Coucouvanis, D.; Simhon, E. D.; Swenson, D.; Baenziger, N. C. *J. Chem. Soc., Chem. Comm.* **1979**, 361–362.

(28) Coucouvanis, D.; Baenziger, N. C.; Simhon, E. D.; Stremple, P.; Swenson, D.; Simopoulos, A.; Kostikas, A.; Petrouleas, V.; Papefthymiou, V. *J. Am. Chem. Soc.* **1980**, *102*, 1732–1734.

(29) Acott, S. R.; Christou, G., Garner, C. D.; King, T. J.; Mabbs, F. E.; Miller, R. M. *Inorg. Chim. Acta* **1979**, *35*, L337–L338.

(30) Cramer, S. P.; Scott, R. A. *Rev. Sci. Inst.* **1981**, *52*, 395–399.

(31) Cramer, S. P.; Hodgson, K. O.; Stiefel, E. I.; Newton, W. E. *J. Am. Chem. Soc.* **1978**, *100*, 2748–2761.

(32) Cramer, S. P. In "EXAFS for Inorganic Systems"; Garner, C. D., Hasnain, S. S., Eds.; Daresbury Laboratory: Daresbury, England WA4 4AD, 1981.

(33) Cramer, S. P.; Solomonson, L. S.; Adams, M. W. W.; Mortenson, L. E. *J. Am. Chem. Soc.* **1984**, *106*, 1467–1471.

(34) Cramer, S. P.; Wahl, R.; Rajagopalan, K. V. *J. Am. Chem. Soc.* **1981**, *103*, 7721–7727.

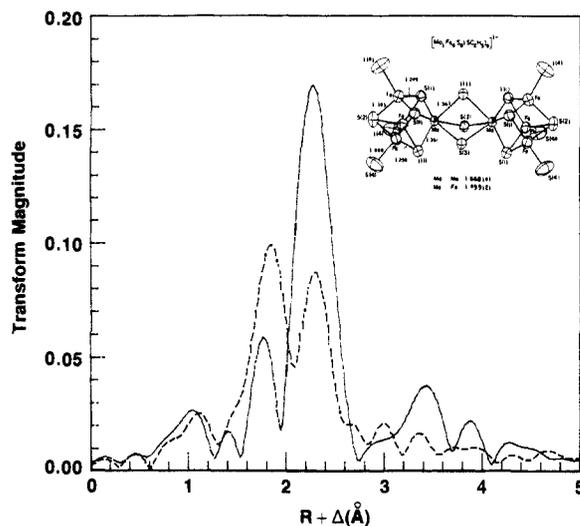(35) Teo, B. K.; Lee, P. A. *J. Am. Chem. Soc.* **1979**, *101*, 2815–2832.

Figure 1. EXAFS Fourier transforms for molybdenum in $(Et_4N)_3$-$[Fe_6Mo_2S_8(SEt)_9]$ single crystal in orientations with 3-fold axis parallel (—) or perpendicular (---) to X-ray polarization. Note the enhanced Mo–Mo peak at $R + \Delta = 3.4$ Å in the parallel orientation. Transform range: 4–14 Å^{-1}, k^3 weighting. Inset: structure of cluster from ref 38.
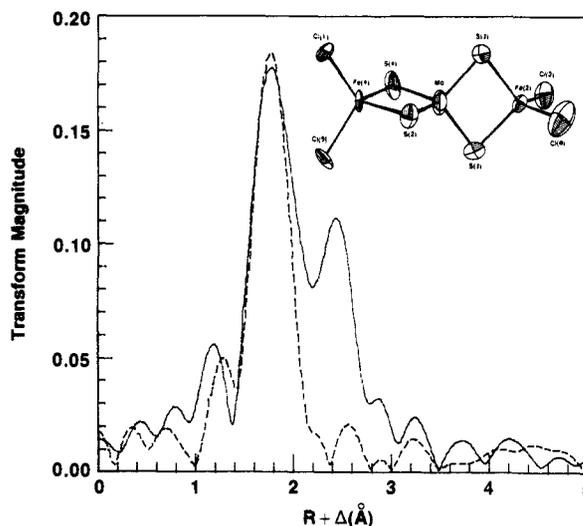

Figure 2. EXAFS Fourier transforms for molybdenum in $(Ph_4P)_2$-$[Cl_2FeS_2MoS_2FeCl_2]$ single crystal in orientations with Mo–Fe axis nearly parallel (—) or perpendicular (---) to X-ray polarization. Transform range: $k = 4$–14 Å^{-1}, k^3 weighting. Inset: structure of cluster from ref 28.

a function of the crystal orientation with respect to the X-ray polarization. Finally, the quality of agreement between the observed and calculated orientation dependence is computed. A listing of the program is included as supplementary material.

Results

Model Compounds. Relatively little work has been done on the single-crystal EXAFS of low molecular weight compounds. It was therefore important to test the experimental accuracy with which such spectra could be measured. Two extreme orientations were recorded for a crystal of the model compound $(Et_4N)_3$-
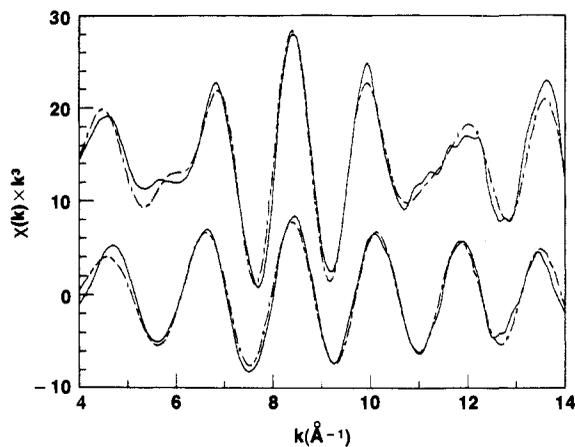
Figure 3. EXAFS for molybdenum in $(Ph_4P)_2[Cl_2FeS_2MoS_2FeCl_2]$ single crystal. Top: observed spectrum (—) and best fit (---) for orientation with maximum Mo–Fe amplitude. Bottom: observed spectrum (—) and best fit (---) for orientation with minimum Mo–Fe amplitude. The top spectrum was shifted vertically by 15 units for clarity.
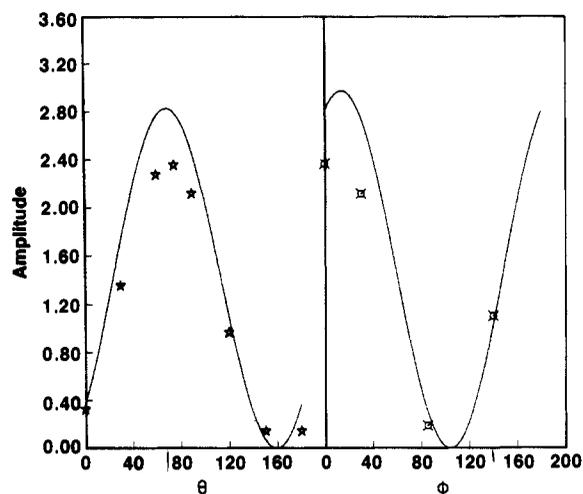

Figure 4. Orientation dependence of Mo–Fe amplitude in EXAFS of $(Ph_4P)_2[Cl_2FeS_2MoS_2FeCl_2]$ single crystal. (a, left) Amplitude as a function of rotation angle θ about the long crystal axis, (star) data points and (—) calculated dependence; (b, right) amplitude as function of rotation ϕ perpendicular to long crystal axis, (cross ed circle) data points and (—) calculated dependence. The calculated curves were derived by adjusting the Mo–Fe axis orientation in the crystal to give the best fit to the data.

$[Fe_6Mo_2S_8(SEt)_9]$, and the EXAFS Fourier transforms are illustrated in Figure 1. As expected, the Mo–Fe component is more intense when the polarization is along the molecular 3-fold axis then when perpendicular to it. The curve-fitting analysis summarized in Table I yielded a factor of 3.2 for the change in Mo–Fe amplitude. For a perfect tetrahedron under optimum polarization and alignment conditions, this ratio would be 4.
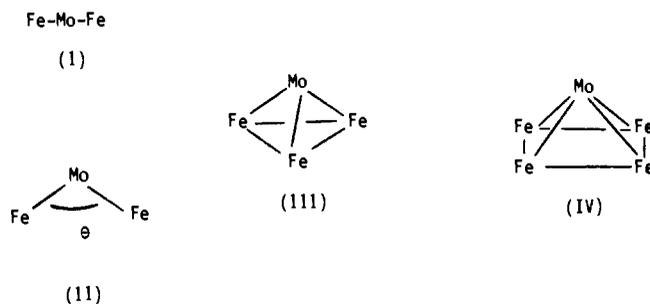
The EXAFS orientation dependence was investigated in more detail for $(Ph_4P)_2[Cl_2FeS_2MoFeS_2Cl_2]$. The EXAFS Fourier transforms, Figure 2, show that the Mo–Fe component can be strongly enhanced or almost completely nullified, depending on the crystal orientation. Curve-fitting the data with variable Mo–S and Mo–Fe amplitudes, as illustrated in Figure 3 and Table I, yielded the Mo–Fe orientation dependence illustrated in Figure 4. The calculated curves were derived by varying the Fe–Mo–Fe axis orientation to obtain the best fit to the data. The Eulerian angles for the orientation of the Fe–Mo–Fe axis derived from the EXAFS ($\alpha = 21.5°$, $\beta = 109°$, $\gamma = 80.5°$) compared favorably with the values ($\alpha = 25°$, $\beta = 110.5°$, $\gamma = 76°$) derived by using an automated diffractometer and the known crystal structure.[28]

Theoretical Calculations. Two distinct types of variables are involved in the interpretation of nitrogenase single-crystal EXAFS—the symmetry of iron neighbors to molybdenum and
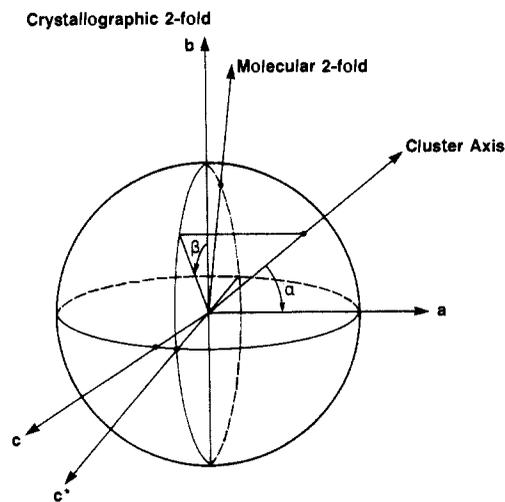
Figure 5. Coordinate system used to describe the orientation of Mo–Fe clusters within the nitrogenase Mo–Fe protein unit cell. The molecular 2-fold axis refers to the nitrogenase molecule, while the cluster axis refers to the axis of highest symmetry passing through molybdenum in the hypothetical cluster.

Scheme II. Mo–Fe Cluster Symmetries Used for Single-Crystal Calculations

the relative orientation of the four molybdenum sites in the unit cell. Without any assumptions about symmetry, there would be from 8 to 16 different Mo–Fe vectors to define, and interpretation of the EXAFS orientation dependence would be overly complicated. However, the problem can be simplified by assuming certain types of symmetry for the nitrogenase unit cell and the Mo–Fe clusters.

X-ray diffraction shows the space group of *Clostridium pasteurianum* MoFe protein crystals to be $P2_1$,[24] with one protein molecule in the asymmetric unit. In this space group, there is a single crystallographic 2-fold rotation axis, defined as the b axis. Although it is not required crystallographically, a self-rotation function analysis has provided good evidence for a molecular 2-fold axis in these crystals at an angle of 20° to the b axis in an orientation which projects onto the c axis in the ac plane.[25] This molecular 2-fold axis presumably relates equivalent sites in the two $\alpha\beta$ dimers which comprise the protein molecule. The data can therefore be analyzed by assuming a particular cluster symmetry, postulating an orientation for one cluster, generating the orientations of the remaining clusters, and comparing the calculated EXAFS variations with the observed data. The cluster symmetries which have been tested are shown in Scheme II, and the coordinate system used for these calculations is illustrated in Figure 5.

In Figure 6a, a comparison is made between the expected orientation dependence for a linear Mo–Fe cluster with two Mo–Fe interactions (structure I) and a tetrahedral cluster of metals with three Mo–Fe interactions (structure IV). To cancel uncertainties about absolute amplitudes, the curves are normalized by the expected powder amplitudes. Although structure III has less anisotropy than structure I, the changes are still a factor of 4 and well within experimental detection limits. Given the presence of four molybdenum sites per unit cell, there was some concern that cluster orientations might exist which would make the EXAFS

Table II. Two-Shell Analyses of Nitrogenase Solution EXAFS

Mo–Fe			Mo–S				
N	R, Å	σ, Å	N	R, Å	σ, Å	F^a	analysis method
3.4	2.67	0.061	4.4	2.34	0.056	0.896	fixed Mo–Fe σ theoretical Fe amplitude
2.3	2.68	0.040	5.2	2.35	0.065	0.856	variable Mo–Fe σ theoretical Fe amplitude
3.9	2.68	0.061	5.0	2.35	0.065	0.982	fixed Mo–Fe σ empirical Fe amplitude
3.1	2.68	0.052	5.5	2.35	0.070	0.968	variable Mo–Fe σ empirical Fe amplitude

^{a} Defined as $[(\chi_{obsd} - \chi_{calcd})^2 k^6/(N_p - N_r)]^{1/2}$, where χ_{obsd} is the observed EXAFS, χ_{calcd} is the calculated EXAFS, N_p is the number of data points, and N_r is the number of parameters refined.
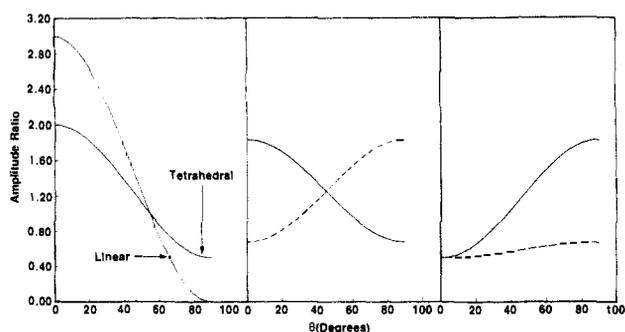

Figure 6. Calculated curves comparing the EXAFS orientation dependence for linar and tetrahedral Mo–Fe clusters. The amplitude ratio plotted in all cases is the expected single-crystal value divided by the powder value. (a, left) Variation in amplitude for a single isolated linear or tetrahedral Mo–Fe cluster as the $\bar{E}$ vector is rotated from parallel to perpendicular to the linear or 3-fold axes, respectively. (b, middle) Variation in amplitude for four tetrahedral Mo–Fe clusters related by the symmetry axes of the Mo–Fe protein unit cell. (—) 3-fold axis of first cluster oriented parallel to molecular 2-fold axis, (---) 3-fold axis of first cluster orientated perpendicular to molecular 2-fold axis. θ is angle of the $\bar{E}$ vector with the b axis where $\bar{E}$ is in the bc^* plane. (c, right) Same as (b), but θ is now defined as the angle of $\bar{E}$ from the a axis where $\bar{E}$ is in the ab plane.

of structure III relatively isotropic. This possibility is addressed in Figure 6b. The calculation uses four tetrahedral clusters, with the orientations of the additional three clusters generated from the symmetry axes. The first cluster 3-fold axis is assumed to be perpendicular or parallel to a protein molecular 2-fold axis and a crystal rotation about the a axis is illustrated. In Figure 6c, the same comparison is made for a rotation about the c^* axis. These figures clearly show how the EXAFS orientation dependence is sensitive to both the symmetry and the orientation of the clusters assumed to be present. Although certain cluster orientations can minimize the EXAFS anisotropy, it cannot be completely eliminated in all directions.

Nitrogenase Solution EXAFS. The original nitrogenase EXAFS interpretation was based on transmission data using lyophilized enzyme and without benefit of Mo–Fe model compounds.[7] Since then, substantial improvements have been made in analysis procedures, fluorescence detection methods,[30] and synthetic model compounds. To take advantage of these developments, a new nitrogenase solution EXAFS spectrum was collected, and the data were analyzed by curve-fitting using theoretical[35] or experimental[33] Mo–Fe amplitudes. The results, which are included in Figures 7 and 8 and Table II, confirm the expectation that the calculated number of iron neighbors is dependent on the type of amplitude function used and assumptions about the Debye–Waller factor. The data are consistent with two, three, or even four iron neighbors at about 2.68 ± 0.03 Å from the molybdenum. Four to six sulfur ligands at an average distance of 2.35 ± 0.03 Å were also found. A small improvement to the fit was achieved by including the presence of one or two nitrogen or oxygen donor ligands at about 2.2 Å. However, the contribution of this component was so small that it was not included in the single-crystal analysis.

Nitrogenase Crystals. The molybdenum EXAFS Fourier transform for solution nitrogenase is compared with the two most
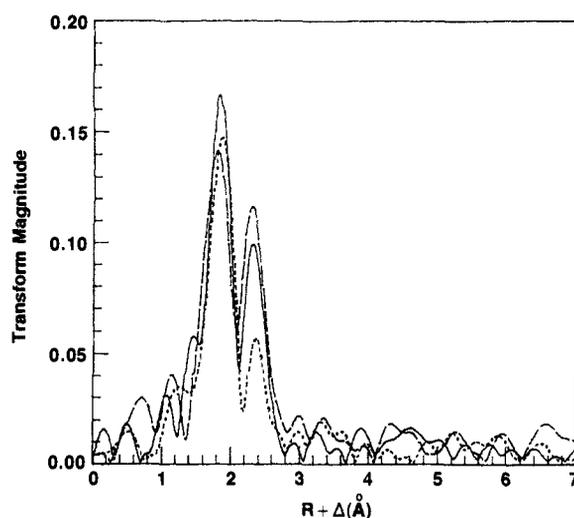

Figure 7. EXAFS Fourier transforms for molybdenum in nitrogenase. Solution data (—) are compared with single-crystal orientations yielding maximum (--) and minimum (---) Mo–Fe amplitudes. Transform range: k = 4–14 Å^{-1}, k^3 weighting.
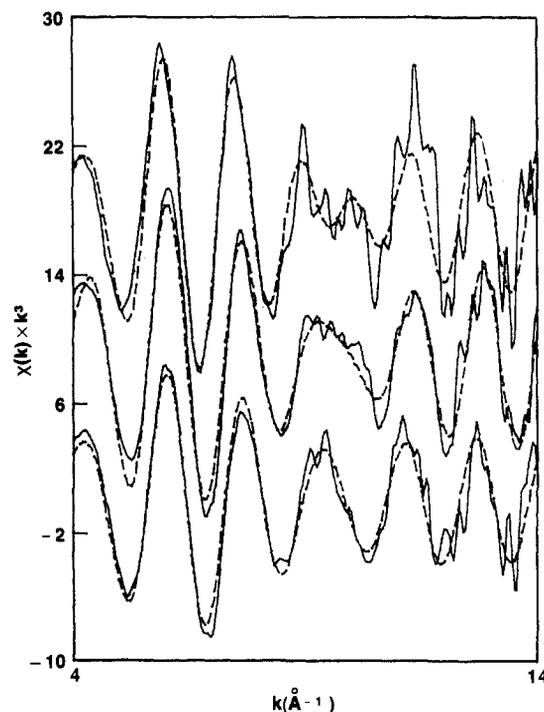

Figure 8. EXAFS for molybdenum in nitrogenase. (Top) observed spectrum (—) and best fit (---) for orientation which gave maximum Mo–Fe amplitude; (middle) observed spectrum (—) and best fit (---) for nitrogenase in solution; (bottom) observed spectrum (—) and best fit (---) for orientation which gave minimum Mo–Fe amplitude.

extreme single-crystal spectra in Figure 7. The Mo–S feature is relatively invariant, whereas there are significant changes in

Table III. Analysis Results for Nitrogenase Single-Crystal EXAFS

| crystal orientation | | | Mo–S | | Mo–Fe | | | | |
| | | | | | exptl | | model | | |
cos $\bar{E}_a$	cos $\bar{E}_b$	cos $\bar{E}_c$[a]	R, Å	N_{xtal}	R, Å	N_{xtal}/N_{soln}	tetrahedral	linear	pyramidal
0.17	0	0.98	2.38	4.0	2.70	1.23	1.28	1.23	1.17
0.17	0.7	−0.66	2.36	4.5	2.69	1.15	1.20	1.41	1.09
0.19	−0.34	−0.72	2.37	4.4	2.69	1.13	0.95	1.12	0.82
0.92	0.087	−0.33	2.36	4.7	2.69	0.56	0.48	0.88	0.90
0.88	−0.044	−0.48	2.37	4.9	2.70	0.88	1.04	1.20	1.03
0	−1	0	2.37	5.0	2.72	0.86	1.03	1.15	0.96
0	0.99	−0.17	2.37	4.7	2.69	1.29	1.01	1.16	0.97
0	0.34	0.94	2.36	4.8	2.69	1.23	1.36	1.46	1.20
−1	0	0	2.37	5.3	2.71	0.74	0.60	0.35	0.80
−0.71	0.71	0	2.39	4.8	2.71	0.53	0.80	0.75	0.88
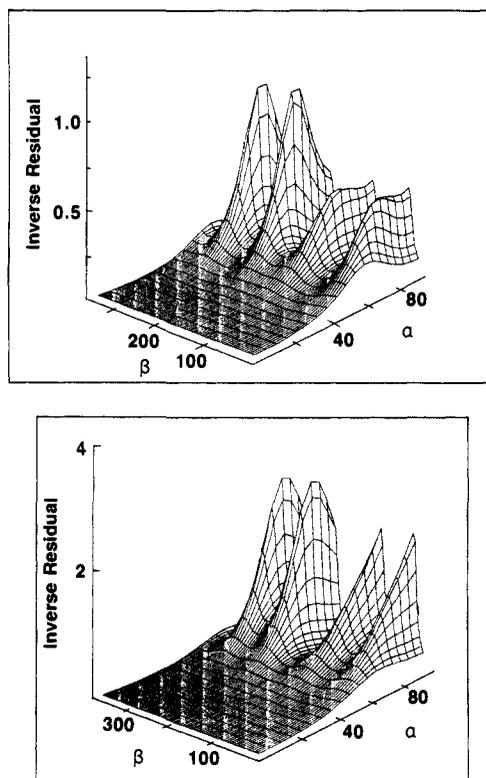
Figure 9. Quality of agreement between the calculated and observed nitrogenase EXAFS orientation dependence, as a function of the orientation of the Mo–Fe cluster axes. Since the reciprocal of the variance is plotted, the best fit occurs at a maximum rather than a minimum. α and β are defined in Figure 5. (a, top) Linear model; (b, bottom) tetrahedral model.

Figure 10. Quality of agreement with experimental results as a function of the bend angle of an Fe–Mo–Fe cluster. The cluster was bent by θ and its orientation was then optimized to give the best fit to the data.

the intensity of the Mo–Fe component. Curve-fitting analysis of these and other EXAFS spectra, as illustrated in Figure 8 and Table III, reveals that the Mo–Fe amplitude changes by a factor of 2.5 from one orientation to another. In contrast, the observed Mo–S amplitude varied by only ±15% in these fits.

The nitrogenase Mo–Fe EXAFS orientation dependence was compared with that expected from the models of Scheme II for a variety of cluster orientations. In the calculations for clusters I, III, and IV, the orientation which needs to be defined is that of the Fe–Mo–Fe, 3-fold or 4-fold symmetry axes, respectively. Rotations of the clusters about the Fe–Mo–Fe symmetry axes do not affect the orientation dependence. In Figure 9, the quality of fit as a function of α and β defined in Figure 5 is illustrated for linear and tetrahedral models. Regardless of the model chosen, the best fit was in the vicinity of $\alpha = 75°$ and $\beta = 215°$ or $285°$. Two different solutions arise because of symmetry; they are related by the molecular 2-fold axis. The broad peaks limit the confidence with which the orientation can be defined to ±10°.

A significantly worse fit was always obtained when a linear Fe–Mo–Fe cluster was assumed, regardless of the orientation in which the cluster axis was placed. This is because the linear cluster
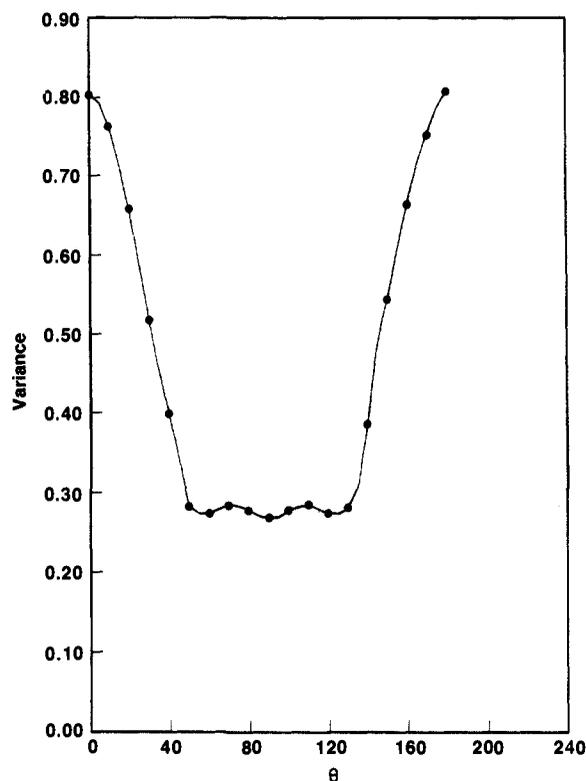
predicts a much greater anisotropy in the EXAFS than is experimentally observed. One way to decrease the EXAFS anisotropy is to bend the cluster as in Scheme II. Therefore, the quality of fit was investigated for this model as a function of the bend angle. As illustrated in Figure 10, the best fit was obtained with a bend angle of 90°. However, a significant improvement was obtained for bent clusters with bend angles between 50° and 130°.

Discussion

Analysis of the new nitrogenase solution data gave results in general agreement with the earlier EXAFS work. With the improved analysis methods, it is simpler to simulate the Mo–S coordination by single component with a relatively large Debye–Waller factor, rather than attempting to resolve two or more distinct Mo–S distances, as was done in previous work.[7,8] However, there is no gaurantee that all the sulfurs are equivalent. The number of iron neighbors remains ambiguous at two to four. This is partly because of the correlation between the calculated coordination number and Debye–Waller factor but also due to uncertainty about transferability of EXAFS amplitudes beyond the first coordination sphere. Finally, the inclusion of one or two nitrogen or oxygen donor ligands at about 2.2 Å does improve the fits. The possibility of some non-sulfur ligands to molybdenum

Single-Crystal EXAFS of Nitrogenase

J. Am. Chem. Soc., Vol. 108, No. 5, 1986 1055

Scheme III. Cluster Symmetries which Have Been Addressed in This Work[a]
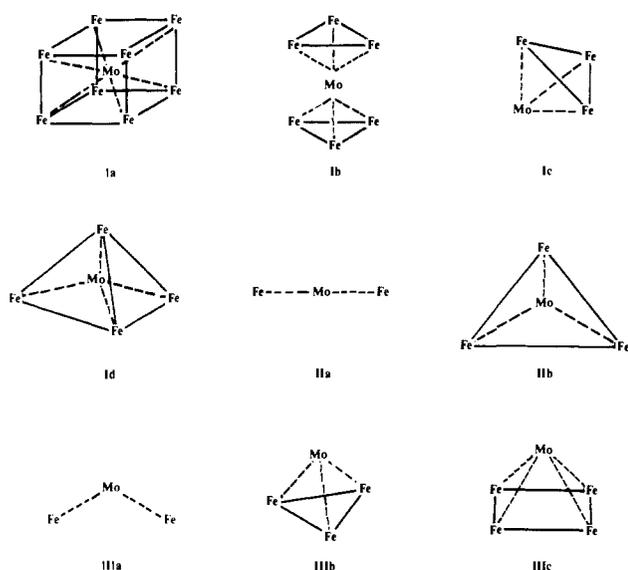
[a] I, clusters which can be eliminated because their EXAFS would be isotropic. II, clusters which can be eliminated because their EXAFS would be too anisotropic. III, clusters with symmetries and calculated EXAFS consistent with the observed data.

should be kept in mind during attempts to synthetically model the FeMo–co cluster.

Before drawing conclusions from the single-crystal results, it is important to consider the errors involved in a single-crystal EXAFS experiment. Possible sources of error in the measurement include incomplete source polarization, crystal imperfections, statistical noise, and inaccurate crystal orientation. Additional errors in the data analysis might also arise if the assumed molecular 2-fold axis is not rigorous. In general, these effects will reduce the ratio between the maximum and minimum EXAFS amplitudes at the extreme orientations.

Independent measurements of the X-ray polarization on other beam lines have yielded polarization ratios of better than 95%,[36] so that this should not be an important effect. The X-ray diffraction results indicate a mosaic spread of less than 1°, so this should also yield only a minor reduction in anisotropy. The signal-to-noise in the protein crystal EXAFS can be estimated by using the fact that the measured Mo–S amplitude varied between 4.0 and 5.3 over the 10 spectra used in the analysis. Some of this variation may in fact be real, but in the worst case, this would indicate an amplitude imprecision of about ±15%. Finally, one of the largest sources of error involves the transfer of different crystals from the precession camera to the goniometer used for the EXAFS experiments. Although better instrumentation is now available, the estimated accuracy of sample orientation is ±5°. With hindsight, it now appears that better results could be obtained by using a single crystal at low temperature for all the experiments.

In this study, it was desired to determine both the orientation and the symmetry of the Mo–Fe cluster in nitrogenase. If the

errors in crystal alignment and Mo–Fe amplitude determination are random, they will reduce the precision of the orientation determination, but there should be no particular orientation that is favored by such errors. With regard to symmetry, experimental errors will reduce the ratio between maximum and minimum Mo–Fe amplitude and thereby reduce the distinction between linear and nonlinear clusters.

Some of the Mo–Fe cluster symmetries which can be addressed by the current investigation are summarized in Scheme III. Despite the experimental limitations imposed by the quality of spectra which can be obtained on small crystals, it is possible to draw several conclusions about the nitrogenase molybdenum site. First of all, the fact that a significant orientation dependence is observed limits the possible symmetry of the arrangement of iron neighbors around the molybdenum. Clusters with no preferred direction, such as Mo at the center of a cube of Fe atoms (Ia), an octahedron of Fe atoms (Ib), a right triangular pyramid (Ic), or molybdenum at the center of a tetrahedron of iron atoms (Id) can be eliminated. All these models can be ruled out because their Mo–Fe EXAFS would be isotropic.

Some types of cluster symmetry can be ruled out by the modest amount of anisotropy which has been observed. The calculations have shown that the linear Fe–Mo–Fe structure (IIa) would have a larger variation in Mo–Fe amplitude than is observed and the same would be expected for a planar triangular structure as in IIb.

Finally, a number of structures, including IIIa–IIIc, are still consistent with the observed EXAFS. Furthermore, the required orientations of the Mo–Fe cluster axes have been approximately located. For clusters IIIa–IIIc, the respective 2-fold, 3-fold, or 4-fold axes are required to lie nearly perpendicular to the *a* axis to be consistent with the observed EXAFS arisotropy. This information should eventually be useful in interpretation of single-crystal EPR effects which have been observed[37] as well as of some help in the X-ray diffraction analysis. More precise orientation should be available in the future by using larger crystals and lower temperatures. When appropriate crystals are available, the higher information content of single-crystal EXAFS will often make it the preferred technique for interpreting metalloprotein local structure.

Supplementary Material Available: Listings of the computer programs used to calculate the orientation dependence of clusters in nitrogenase crystals (37 pages). Ordering information is given on any current masthead page.

(36) Templeton, D., personal communication.

(37) Mortenson, L.; Adams, M., work in progress.
(38) Wolff, T. E.; Berg, J. M.; Hodgson, K. O.; Frankel, R. B.; Holm, R. H. *J. Am. Chem. Soc.* **1979**, *101*, 4140–4150.